International Journal of Heat and Mass Transfer 52 (2009) 4919–4928

Contents lists available at ScienceDirect

International Journal of Heat and Mass Transfer

journal homepage: www.elsevier.com/locate/ijhmt

Dilution and hydrate forming process in shock waves

V.E. Dontsov *, A.A. Chernov

Kutateladze Institute of Thermophysics, SB RAS, Novosibirsk 630090, Russia

ARTICLE INFO

Article history:
Received 15 August 2008
Accepted 24 April 2009
Available online 6 July 2009

Keywords:
Shock wave
Fluid
Gas bubble
Bubble fragmentation
Dilution
Hydrate forming
Surfactant

ABSTRACT

Process of dilution and hydrate forming beyond the front of the shock wave with moderate amplitude (moderate shock wave front) in water with carbonic gas bubbles at varying initial static pressures has been experimentally observed and studied. Influence of surfactants on dilution and hydrate forming process beyond the shock wave occurring in the medium has been scrutinized. It has been proved that beyond the moderate shock wave in fluid with carbonic gas bubbles intense process of dilution and hydrate forming occurs resulting in complete loss of gas phase for several milliseconds. Surfactants present in the medium proved to be insignificant for dilution and hydrate forming process in the studied time range. Dependence of dilution and hydrate forming process beyond the shock wave from wave and medium parameters has been revealed. Theoretical model of dilution and hydrate forming process beyond the shock wave in gas and fluid medium taking into account convective and molecular gas diffusion in fluid, convective and conductive heat exchange caused by heat release in interphase boundary resulted from dilution and hydrate forming has been offered. Close fit of experimental data and calculations has been achieved.

1. Introduction

One of the important factors of the changing climate is the increase of carbon dioxide in the Earth atmosphere. Due to the increasing commercial production in Russia atmospheric emission of carbon dioxide in the nearest future will significantly grow resulting in the emerging problem of its reduction in accordance with the provisions of the Kyoto Protocol. At present various technologies for carbonic gas utilization are proposed. One of the prospective methods of utilization is transfer of gas into gas hydrate state and its storage on the ocean floor at the lower temperature and high static pressure [1–5]. One of the main parameters providing for economic expedience of such method is the velocity of carbonic gas hydrate forming. There are various methods to intensify gas hydration process: fine atomization of the fluid saturated jet in the gaseous atmosphere [6–8], intense agitation of water saturated with dissolved gas [7,9], vibratory impact on gas enriched fluid [11], ultrasonic influence on the medium [12], etc. Main disadvantage of the proposed methods is low velocity of hydrate forming resulting in low productivity of plants constructed on the basis of these methods.

Authors [13] have suggested innovative shock-wave method to intensify gas hydrate forming process. It has been demonstrated that main mechanism intensifying hydrate forming process is gas bubbles fragmentation in the shock wave. In the paper [14,15], dilution and hydrate forming process beyond medium shock wave in water with Freon 12 bubbles at static atmospheric pressure has been experimentally studied. Kinetic model of hydrate forming beyond the step profile shock wave in fluid and gas medium allowing to ignore thermal effects has been proposed. In the paper [16], shock wave evolution in gas and fluid medium taking into account gas bubbles fragmentation, dilution and hydrate forming process beyond the shock wave has been studied. It was demonstrated that increase of static pressure in gas and fluid medium results in the decrease of relative amplitude of the shock wave causing the development of Kelvin–Hemholtz instability and bubbles fragmentation into small gas occlusions beyond the shock wave.

In the works [17–21], influence of various surfactants on the velocity of hydrate forming in the static medium under the condition of intense medium agitation and liquid atomization in gas phase has been experimentally studied. It was demonstrated that surfactants present in water result in the increased velocity of gas hydrate forming. Authors have proposed mechanisms to intensify hydrate forming process by surfactants.

In this work dilution and hydrate forming beyond the shock wave in water with carbonic gas bubbles at various initial static pressures have been experimentally studied. Influence of medium surfactants concentration onto the process of dilution and hydrate forming has been studied. Theoretical model of dilution and hydrate forming process beyond the shock wave in gas and fluid medium taking into account convective and molecular gas diffusion in fluids, convective and conductive heat exchange resulted from heat generation in the interphase boundary has been proposed.

---

* Corresponding author. Tel.: +7 383 316 50 38; fax: +7 383 330 84 80.
E-mail addresses: dontsov@itp.nsc.ru (V.E. Dontsov), chernov@itp.nsc.ru (A.A. Chernov).

0017-9310/$ - see front matter © 2009 Published by Elsevier Ltd.
doi:10.1016/j.ijheatmasstransfer.2009.04.030

Nomenclature

a	fluid thermal diffusivity ratio [m^2/s]
D	fluid diffusion ratio [m^2/s]
j_s	density of gas flow from bubble into fluid (dilution) [kg/(m^2 s)]
j_h	density of gas flow from bubble into hydrate envelope [kg/(m^2 s)]
K	kinetics coefficient [m/(s K)]
L_h	specific heat of hydrate forming [kJ/kg]
L_s	specific heat of dilution [kJ/kg]
M	mass concentration of dissolved gas in fluid volume unit [kg/m^3]
m	mass concentration of surfactant in water [ppm]
m_h	mass concentration of gas in hydrate [kg/kg]
m_{cl}	mass of substance involved in motion by fluid and gas cluster [kg]
m_b	mass of substance involved in motion by the bubble in cluster[kg]
Nu	Nusselt number = $\alpha R_b/\lambda$
Pe	Peklet number = $V_b R_b/a$
Pe_D	Peklet diffusion number = $V_b R_b/D$
P_0	initial medium pressure [MPa]
P_1	medium pressure beyond the shock wave front [MPa]
ΔP	shock wave amplitude [MPa]
P_s	equilibrium pressure of hydrate forming [MPa]
q_T	density of heat flow [kJ/(m^2 s)]
q_s	heat generation in the surface unit of the bubble resulted from dilution [kJ/(m^2 s)]
R	initial radius of the bubble [m]
R_{cl}	cluster radius [m]
R_b	cluster bubble radius [m]
R_c	cluster bubble radius following isothermal compression in the wave front [m]
Re	Reynolds number = $2R_b\rho_l V_b/\mu_l$
Sh	Sherwood number = $\beta R_b/D$
T	fluid temperature [°C]
T_s	hydrate forming equilibrium temperature [°C]
T_R	temperature at interphase boundary [°C]
T_c	critical temperature of carbonic gas hydrates forming [°C]
t	time [s]
V	gas bubbles velocity (until fragmentation) with regard to fluid beyond the shock wave [m/s]
V_b	gas bubbles velocity (until fragmentation) with regard to cluster beyond the shock wave [m/s]
V_{cl}	cluster velocity with regard to fluid beyond the shock wave [m/s]
We	Weber's number = $(2R\rho_g V^2)/\sigma$

Greek symbols

α	heat emission ratio = $q_T/\Delta T$ [kJ/(m^2 s K)]
β	mass transfer ratio = $j_s/\Delta M$ [m/s]
Δ	thickness of hydrate envelope around gas bubble [m]
λ	fluid heat conductivity ratio [kJ/(m s K)]
μ_l	fluid dynamic viscosity [Pa s]
ρ_g	gas density in the bubble [kg/m^3]
ρ_l	fluid density [kg/m^3]
ρ_h	hydrate density [kg/m^3]
σ	surface tension of fluid [N/m]
τ_s	time of gas bubbles dilution in fluid [s]
τ_{h+s}	time of concurrent process of gas dilution and hydration [s]
φ	volumetric gas content in fluid [%]
φ_{cl}	initial volumetric gas content in cluster [%]
φ_c	volumetric gas content in fluid following isothermal bubble compression in the wave front [%]
φ_*	measured value of volumetric gas content in time t = 9 ms beyond the shock wave front [%]

Indexes

0	medium parameter value prior to the shock wave
R	medium parameter value in the boundary of the gas bubble

2. Experimental setup

Experiments were carried out on the "shock tube" setup (Fig. 1). Work section was set up as vertical heavy-wall steel tube with internal diameter of 53 mm and 1.5 m long limited from below by the heavy wall. The work section was fulfilled with water under vacuum that allowed avoiding air bubbles in the fluid. Fluid in the bottom of the work section along its perimeter was supplied with gas bubbles through the holes with the diameter of 0.6 mm. As the gas phase carbonic gas was used. Such method of bubbles supply served to achieve large enough volumetric gas content. Average radius of bubbles ranged from 2 to 3 mm. As the operative fluid researches used weak solution of sodium chloride in water (with salinity of 0.5 g/l), enriched by carbonic gas to equilibrium state under given initial conditions (temperature and static pressure) with different concentration of surfactants. *n*-Octanol alcohol was used as surfactant. Experiments were carried out with mass concentration of the surfactant equal to 0, 100 and 400 ppm. The lattermost concentration value is close to the peak concentration of surfactant under the studied temperatures when surfactant is completely water-soluble. Initial static pressure in gas and fluid medium ranged in the limits of $P_0 = (0.5–1.3)$ MPa. To keep necessary static pressure in the medium strain sensor-driven and located in the work section electromagnetic valve was used. The work section was thermostated by flushing of the coolant between its external wall and jacket. From outside the jacket was covered with the thermoisolating material. To flush the coolant thermostat with refrigerator was applied. Fluid temperature in the work section was changed by two thermocouples set in the upper and lower parts of the work section. Experiments were carried under the medium temperature of T_0 = 10 and 1 °C. Average initial gas content φ_0 on the work section length was identified against measuring of the spout rise in the work section in the time of gas bubbles supply. Bubble size was determined by shooting with digital camera supplied with additional optics, through the optic glass in the upper part of the work section.

Echelon form pressure waves were formed by the diaphragm breach dividing high-pressure chamber of 2 m long and work section. During the diaphragm exchange the work section was shut down by ball cock to avoid depressurization and fluid degas. Ball cock with internal diameter equal to the one of the work section was placed in its upper part. Pressure wave profiles were registered by pressure piezoelectric detector and strain sensor, located along the work section and embedded in its internal wall. To measure the local profile of gas content beyond the medium shock wave, conductivity indicator was made up in the non-conductive tube with square cut which faces slipped into round cut equal to the work section cut. Electrodes of the conductivity sensor were embedded in the internal wall of the tube with square cut which allowed generating homogenous electrical field in the area of measuring. Besides, sensor electrodes gave no distortion of the medium flow beyond the wave and the sensor served to measure gas con-

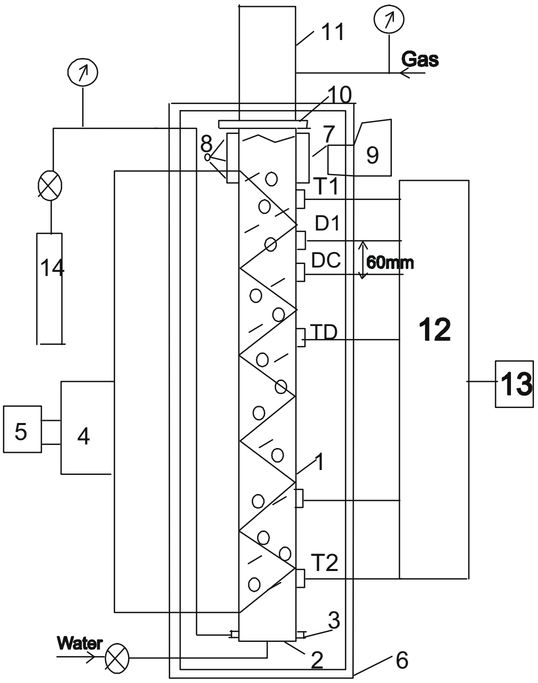

Fig. 1. Scheme of experimental setting. 1 – work section, 2 – work section bottom, 3 – gas bubble generator, 4 – thermostat, 5 – coolant, 6 – thermoisolator, 7 – optical window, 8 – flashbulb, 9 – optical system, 10 – diaphragm, 11 – high-pressure chamber, 12 – ADC, 13 – computer, 14 – gas cylinder, D1 – pressure piezoelectric detector, T1, T2 – thermocouples, TD – strain sensor, DC – conductivity sensor.

tent profiles beyond the wave with large enough amplitude. Conductivity sensor was located in the upper part of the work section measuring average volumetric gas content under cut and height of 20 mm. Specific averaging time of volumetric gas content in the wave conductivity sensor depended on the wave passing through the sensor and amounting to less than 0.2 ms. Distance between pressure piezoelectric detector and conductivity sensor was 60 mm. Signals from the sensors were supplied to ADT and were processed by the computer.

3. Theoretical analysis

Consider fluid (water enriched with gas to equilibrium state at the given temperature and pressure) with gas bubbles and diffusive one-dimensional step profile shock wave. Assuming that in the wave front bubbles are atomized into small gas occlusions forming gas and fluid clusters. Since fluid beyond the wave front turns out to be in the undersaturated state process of gas dilution in fluid starts. Consider situation when medium beyond the shock wave front turns out to be in one of the phase states allowing for hydrate forming. It results in forming and growth of hydrate envelopes in the boundary of gas bubbles. Work [22] stated that hydrate formed on the surface of the gas bubble moving in water grows in the form of separate crystals (crystal-wise). It was noticed that hydrate crystal film is a minor obstacle for interaction of gas and water and there is always free surface for gas and fluid contact. Therefore we can assume that concurrent process of dilution and hydrate forming beyond the shockwave front is mainly determined by heat and mass output in the interphase boundary, and diffusion through the hydrate envelope can be ignored.

Assumptions made during the development of this theoretical model are as follows. Gas bubbles after fragmentation form gas and fluid clusters of spherical shape containing small gas occlusions equal in size and also spherical in shape. Gas and fluid clusters attain initial speed in the wave front with regard to fluid and then are retarded because of dynamic resistance and viscous friction [23]. Accordingly, relative motion of gas occlusions appears in cluster resulting in convective heat and mass exchange in the interphase boundary. Hydrate is formed on the interphase surface, grows radially and has no impact on dilution process. To describe process of heat and mass exchange we use quasi-static settlements and consider time of attainment of static mode as small compare to specific time of the overall process. Besides, diffusive interaction of the bubbles in cluster is not taken into account since distance between neighboring bubbles far exceeds specific thickness of diffusive boundary layers formed around each bubble. Solving heat task the authors took into account change of fluid temperature in the cluster during dilution and hydrate forming process.

Taking into account abovementioned assumptions draw up the equation of material balance describing changes of gas mass in the bubble conditioned by dilution and hydrate forming

$$\rho_g dR_b/dt = -(j_s + j_h), \tag{1}$$

where R_b – the bubble radius, ρ_g – gas density in the bubble, j_s – density of gas flow from the bubble to fluid (dilution), j_h – density of gas flow from the bubble to hydrate envelope. The latter in Eq. (1) in connected with the increase of hydrate mass as follows:

$$\rho_h d\Delta/dt = j_h/m_h, \tag{2}$$

where Δ – thickness of hydrate envelope around the bubble, ρ_h – hydrate density, m_h – mass concentration of gas in hydrate. Note that gas density in the bubble is far less than hydrate density and the hydrate envelope thickness remains for the whole hydration time (except for the last stage) far less than the size of the bubble itself.

Eqs. (1) and (2) should be supplemented with the energy balance equation determining the velocity of hydrate envelope growth

$$L_h \rho_h d\Delta/dt = q_T - q_s, \tag{3}$$

where L_h – specific heat of hydrate forming, q_T – density of the heat flow, $q_s = L_s j_s$ – heat on the bubble surface unit resulted from dilution, L_s – specific heat of dilution. In case, when q_T is less q_s, hydrate growth stops and the process of pure dilution described by the following Eq. (1) c $j_h = 0$ proceeds.

Heat and mass emission from the bubble moving in fluid are described by the following criterial equations [24]

$$Nu = \sqrt{2/\pi} Pe^{1/2} + 1, \tag{4}$$

$$Sh = \sqrt{2/\pi} Pe_D^{1/2} + 1, \tag{5}$$

where $Nu = \alpha R_b/\lambda$ – Nusselt number, $Sh = \beta R_b/D$ – Sherwood number, $Pe = V_b R_b/a$ – Peklet number, $Pe_D = V_b R_b/D$ – Peklet diffusive number, $\alpha = q_T/\Delta T$ – heat emission ratio, $\beta = j_s/\Delta M$ – mass transfer coefficient, $\Delta T = T_R - T_0$, $\Delta M = M_R - M_0$. T – fluid temperature, M – mass concentration of the dissolved gas in the fluid volume unit. Index «*0*» denotes medium parameter value prior to the shock wave and «*R*» – in the boundary of the gas bubble. λ, D, a – accordingly heat conductivity, diffusion and thermal diffusivity coefficients, V_b – gas bubbles velocity on regard to the cluster beyond the shock wave. The first member in the right part of the Eqs. (4) and (5) accounts for convective, the second one for conductive constituents of heat and mass transfer. It is shown that in the course of time the second member in these equations beyond the wave front becomes predominant due to fast retardation of the bubble in fluid.

Note that temperature value on the bubble surface has not been identified and equation set (1)–(5) should be supplemented with kinetic equation: $d\Delta/dt = K(T_s - T_R)$, where K – kinetic coefficient. However, as calculations show temperature in the interphase boundary T_R rather quickly (for times far less than specific time of the process) for the studied parameters of waves and medium verges toward the equilibrium temperature of the phase change T_s. Therefore, hydrate forming kinetics influences the process only in the initial stage of hydrate growth.

Note that Eqs. (4) and (5), and values of heat and mass flows are averaged over the bubble surface. However, considering that specific solutions (angular dependence) for the equations of heat and mass transfer are identical, use of averaged dependences in this task is rather accurate and proper.

To close the equation set we used the equation of motion of gas and fluid cluster and gas bubble in cluster beyond the shock wave [23]

$$dV_{cl}/dt = -f_{cl}/m_{cl}, \tag{6}$$

$$dV_b/dt = 2dV_{cl}/dt - f_b/m_b, \tag{7}$$

where V_{cl} – velocity of cluster motion with regard to fluid beyond the shock wave, $f_{cl,b} = C_\mu \pi R^2_{cl,b}\rho_l V^2_{cl,b}/2$ – resistance force affecting cluster (index cl) and bubble (index b), $C_\mu = 24/\mathrm{Re} + 4/\sqrt{\mathrm{Re}} + 0.4$, $\mathrm{Re} = 2V_bR_b\rho_l/\mu_l$ – Reynolds number, ρ_l – fluid density, μ_l – fluid dynamic viscosity, m_{cl} and m_b – mass of substance involved into motion by cluster and bubble in cluster accordingly. Mass of cluster is composed from mass of gas and fluid in cluster plus fluid mass, and bubble mass – from mass of gas in the bubble, hydrate envelope mass plus fluid mass.

In the process of dilution and hydrate forming beyond the shock wave value of bulk concentration of bubbles in fluid φ will be described by the ratio $\varphi/\varphi_c = (R_b/R_c)^3/(1-\varphi_c(1-(R_b/R_c)^3))$, where φ_c and R_c – accordingly volumetric gas content and bubble radius after isothermal compression of gas bubbles in the wave front.

Presented set of equations completely determine dilution and hydrate forming process beyond the wave front spread in the fluid with gas bubbles. In the calculations we used dependences of carbonic gas solubility from pressure and temperature [25], dependence of equilibrium temperature of carbonic gas hydrate forming from pressure [26] and value of hydrate forming heat and carbonic gas dilution [26,27].

4. Results of experiment, comparison with calculations

Influence of surfactant on dilution and hydrate forming beyond the shock wave in gas and fluid mixture has been studied. Earlier in works [14–16] it was demonstrated that owing to gas bubbles fragmentation and significant increase of interphase surface beyond the shock wave process of gas dilution in fluid and hydrate forming is intensified. Process of gas bubble fragmentation beyond the shock wave in gas and fluid medium results from Kelvin–Helmholz instability caused by relative motion of gas bubbles and is determined by Weber's number $We = (2R\rho_g V^2)/\sigma$. σ – fluid surface tension. Therefore, surfactant supplemented into fluid decreases surface tension that should result in gas bubble fragmentation beyond the wave into smaller gas occlusions in pari causa and accordingly in intensification of dilution and hydrate forming.

Another mechanism to intensify hydrate forming beyond the shock wave in gas and fluid medium by surfactant is possible. In the paper [19], it was shown that addition of surfactant into water results in displacement of equilibrium curve of hydrate forming. That is at the given temperature addition of surfactant results in the decreased equilibrium pressure of hydrate forming. Therefore, in this case surfactant present in the medium also can result in intensification of hydrate forming.

The authors can propose one more mechanism to intensify hydrate forming by adding surfactant into the medium. It is known that for surfactant molecules in gas and fluid the energy optimum is to accumulate in the interphase boundary therefore their concentration at the boundary is high. Besides large concentration of surfactant in the interphase boundary serve to form clusters from surfactant molecules. Thus, surfactant in the boundary can serve extra heterogeneous nuclei for gas-hydrate growth.

Fig. 2 shows experimental profiles of pressure wave (line 1) and local volumetric gas content in the wave (line 2) at the static pressure P_0 = 0.5 MPa, medium temperature T_0 = 10 °C and different mass concentration of surfactant m in water. Since at the given temperature gas hydrates forming process does not occur (critical temperature of carbonic gas hydrate forming T_c = 10 °C), therefore carbonic gas content in fluid beyond the shock wave is determined only by gas compressibility and dilution. Line 3 demonstrates the calculated value of isothermal compression of gas bubbles in the shock wave – $\varphi_c = \varphi_0(\varphi_0 + (1-\varphi_0)P_1/P_0)^{-1}$. $P_1 = P_0 + \Delta P$ – pressure beyond the shock wave front. Line 4 – calculated profile of gas content according to the proposed model. As it was demonstrated above [16], beyond the medium shock wave in water with gas bubbles there is the process intense dilution of carbonic gas conditioned by bubbles fragmentation – Fig. 2a and b. Comparison of gas content profiles on Fig. 2a and b shows that there is strong dependence of dilution velocity from the wave amplitude. Less than 10% change of amplitude results in significant increase of velocity of carbonic gas dilution in water. For relative wave amplitudes $\Delta P/P_0 \sim 5$ during 10 ms carbonic gas almost completely dissolves in water.

Note that discrepancy of pressure wave front and volumetric gas content on the presented figures are conditioned by continuous in-line arrangement of sensors in the work section of the shock tube.

Fig. 2c and d demonstrates profiles of waves and gas contents at the mass concentration of surfactant in water m = 100 ppm, Fig. 2e and f – m = 400 ppm. At100 ppm concentration of n-octanol in water medium surface tension decreases to ~30%, at 400 ppm – approximately 2.5 times [28]. Comparing profiles of gas content for different surfactant concentration and close values of wave amplitudes (Fig. 2b–f) we come to a conclusion that presence of surfactant in the medium does not lead to significant change of gas content profiles and therefore to changes in velocity of carbonic gas dilution in water. Thus, above proposed mechanism of intensification of gas dilution beyond the shock wave by means of surfactants does not work. The reason can be as follows. Under fragmentation of gas bubbles beyond the shock wave interphase surface increases over an order. Accordingly, surfactant concentration on the interphase surface significantly decreases during fragmentation and surfactant stops being effective. We evaluated time of reconstruction of surfactant concentration on the interphase surface (time of egression of surfactant molecules in the interphase boundary), that is several tens of milliseconds. Therefore, for the period of gas bubbles fragmentation (less than a millisecond for the studied wave amplitudes), surfactant concentration in the interphase boundary has insufficient time for reconstruction. Accordingly, surface tensions in the interphase boundary for the medium without surfactants and with them for studied times will not differ significantly.

Comparison of experimental profiles of gas content (line 2) with calculation lines (line 4) demonstrates that proposed theoretical model well describes gas dilution process beyond the shock wave front in gas and fluid medium – Fig. 2. In the calculations radius of bubbles in cluster was chosen in accordance with the experiment and the initial volumetric gas content in gas and fluid cluster was φ_{cl} = 50%. If radius of bubbles in the cluster significantly influences on gas content profile in the process of gas dilution beyond the wave front, φ_{cl} practically has no influence on the dilution process. At the initial stage of dilution there is minor deviation of calculated profiles (line 4) from experimental ones (line 2) occurring parallel to wave amplitude growth. This can be caused by durability of gas bubbles fragmentation process which within the experiment takes some time during the time interval beyond the wave

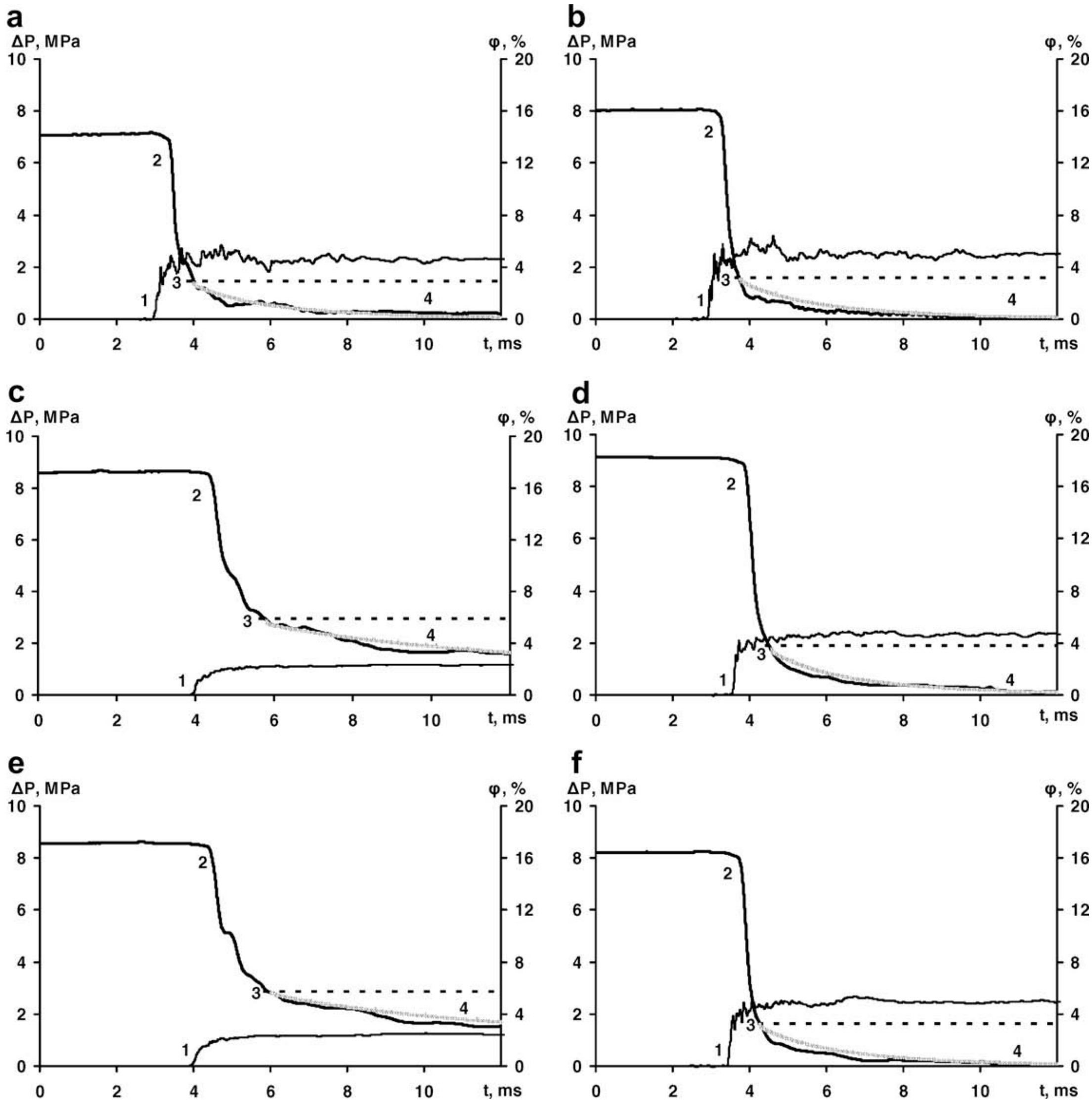

Fig. 2. Profiles of pressure shock wave and volumetric gas content in the wave in terms of gas dilution. P_0 = 0.5 MПa, T_0 = 10 °C. (a) m = 0 ppm, ΔP = 2.3 MPa, φ_0 = 14.3%; (b) m = 0 ppm, ΔP = 2.45 MPa, φ_0 = 16.1%; (c) m = 100 ppm, ΔP = 1.17 MPa, φ_0 = 17.3%; (d) m = 100 ppm, ΔP = 2.35 MPa, φ_0 = 18.4%; (e) m = 400 ppm, ΔP = 1.21 MPa, φ_0 = 17.1%; (f) m = 400 ppm, ΔP = 2.45 MPa, φ_0 = 16.5%.

front. In this case contribution to gas dilution because of radial relative motion of gas bubbles in cluster during fragmentation with increased wave amplitude can be significant.

Fig. 3 demonstrates experimental profiles of pressure wave (line 1) and local volumetric gas content in the wave (line 2) at the static pressure P_0 = 0.5 MPa, medium temperature T_0 = 1 °C and various mass concentrations of surfactant m in water (3 – line of isothermal compression of gas bubbles, 4 – calculation profile of gas content according to the proposed model). This temperature corresponds with equilibrium pressure of carbonic gas hydrate forming equal to $P_s \sim 1.38$ MПa [26]. Therefore, in gas and fluid medium beyond the shock wave with $P_1 > P_s$ hydrate forming is possible. As it was mentioned above [16], decrease of medium temperature can cause rise of hydrate forming beyond shock wave of medium amplitude. In fact, comparing profiles of gas content in water without surfactants for different temperatures (Fig. 2a and Fig. 3a) we have velocity of gas content decrease beyond the wave at T_0 = 1 °C higher than at T_0 = 10 °C. This results from increased carbonic gas solubility in water caused by the decrease of medium temperature and hydrate forming process.

Fig. 3b and c shows profiles of waves and gas contents at mass concentration of surfactant in water m = 100 ppm, and Fig. 3d and e – m = 400 ppm for different values of wave amplitudes. Comparing profiles of gas contents for different values of surfactant concentration and close values of wave amplitudes (Fig. 3a–e) we reveal that presence of surfactant in the medium does not result in significant changes in gas content profiles and therefore to changing dilution and hydrate forming velocities. Thus, above proposed mechanisms of intensification of gas dilution and hydrate forming by surfactant do not work. Mechanisms of surfactants influence on hydrate forming connected with displacement of equilibrium curve and forming of additional centers of hydrate forming are not effective because of insufficient concentration of surfactant in the interphase boundary beyond the shock wave for the studied times.

Comparison of experimental profile of gas content (line 2) with calculation lines (line 4) shows that proposed theoretical model well describes concurrent process of gas dilution and hydrate forming beyond the shock wave front in gas and fluid medium – Fig. 3. In calculations initial volumetric gas content in gas and fluid

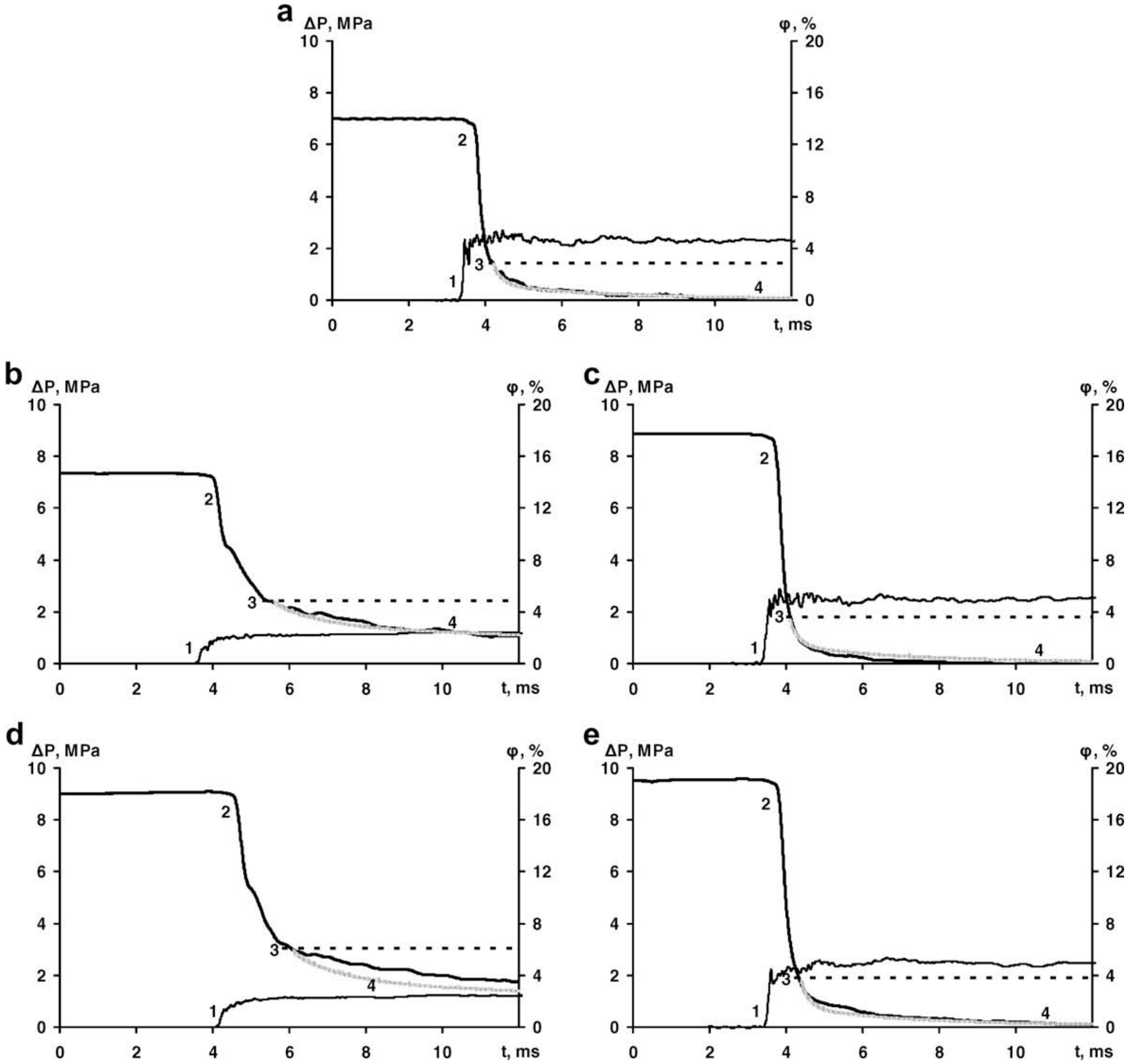

Fig. 3. Profiles of pressure shock wave and volumetric gas content in the wave in terms of gas dilution and hydration. $P_0 = 0.5$ MPa, $T_0 = 1$ °C. (a) $m = 0$ ppm, $\Delta P = 2.31$ MPa, $\varphi_0 = 13.9\%$; (b) $m = 100$ ppm, $\Delta P = 1.2$ MPa, $\varphi_0 = 14.7\%$; (c) $m = 100$ ppm, $\Delta P = 2.4$ MPa, $\varphi_0 = 17.7\%$; (d) $m = 400$ ppm, $\Delta P = 1.22$ MPa, $\varphi_0 = 18.1\%$; (e) $m = 400$ ppm, $\Delta P = 2.5$ MPa, $\varphi_0 = 19.0\%$.

cluster was $\varphi_{cl} = 50\%$. Note, that hydrate forming process plays main role in changing gas content beyond shock wave front in the initial section of calculated profiles 4 – Fig. 3, whereas the completion stage of studied process is determined mainly by dilution of gas in fluid.

Fig. 4 shows experimental profiles of pressure wave (line 1) and local volumetric gas and fluid content in the wave (line 2) at static pressure $P_0 = 1.3$ MPa, medium temperature $T_0 = 10$ °C and various mass concentrations of surfactant m in water. Since at the given temperature gas-hydrate is not formed therefore carbonic gas content in fluid beyond the shock wave is determined only by gas compression and dilution. Line 3 presents calculation for isothermal compression of gas bubbles beyond the shock wave and line 4 – calculation according to the model. Comparing experimental profiles of gas content for different values of surfactant concentration and close values of wave amplitude (Fig. 4a and d), we infer that presence of surfactant in the medium does not cause significant changes of gas content profiles and therefore change in velocity of carbonic gas dilution in water. Thus, also at the given static pressure surfactant does not speed up gas dilution process beyond the shock wave.

Note that increase of static pressure in gas and fluid medium results in gas bubbles fragmentation at lesser relative wave amplitudes $\Delta P/P_0$ [16]. Therefore, as the static pressure grows at the constant relative wave amplitude, velocity of gas dilution in fluid increases because of the decrease of gas oscillation size. In fact comparing gas content profiles at different static pressures in Figs. 4a and d, and 2c and e it can be inferred that dilution process at $P_0 = 1.3$ MPa (even for lesser relative amplitudes $\Delta P/P_0$) is more intense than at $P_0 = 0.5$ MPa.

Comparison of experimental gas content profiles (line 2) with calculation lines (line 4) shows that theoretical model rather well describes gas dilution process beyond the wave front with amplitude $\Delta P/P_0 \leqslant 2$ ($\varphi_{cl} = 50\%$) – Fig. 4a, b and d. Experimental profile in Fig. 4c is much lower than calculated dilution curve. It may result from significant influence of carbonic gas liquefaction beyond the strong shock wave front. At the medium temperature $T_0 = 10$ °C equilibrium pressure of carbonic gas equilibrium is 4.5 MPa [26]. During further improvement of the model process of gas liquefaction beyond the shock wave will be taken into account.

Fig. 5 presents shows experimental profiles of pressure wave (line 1) and local volumetric gas and fluid content in the wave (line

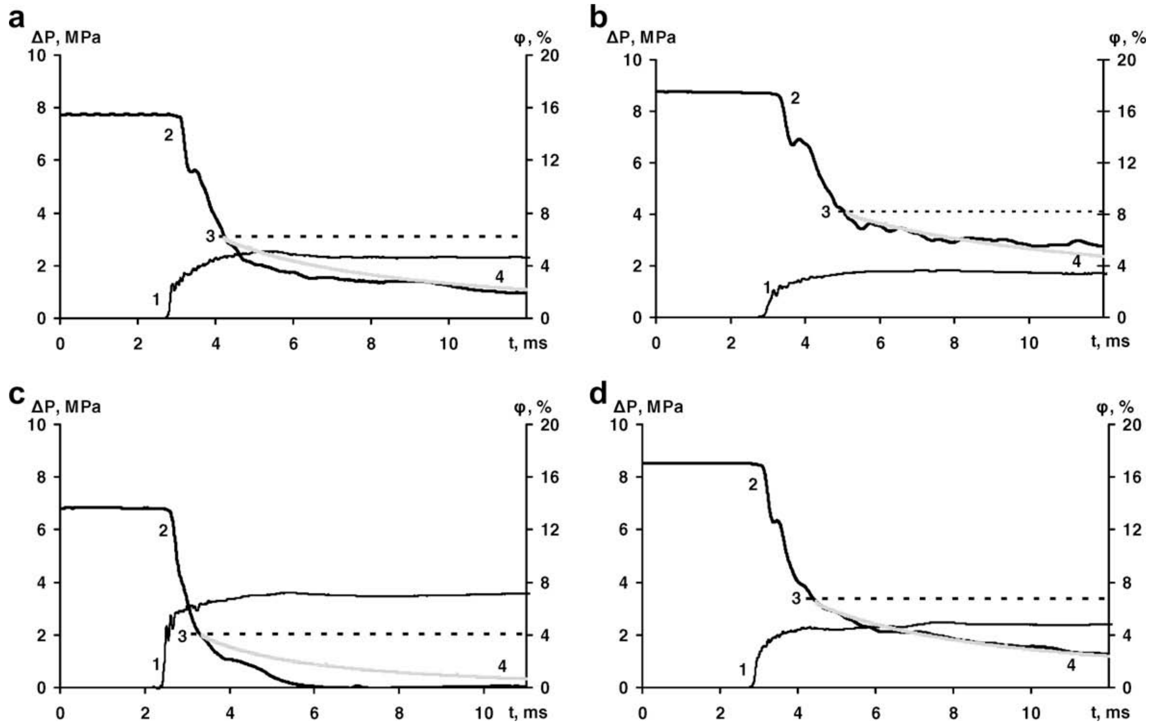

Fig. 4. Profiles of pressure shock wave and volumetric gas content in the wave in terms of gas dilution. $P_0 = 1.3$ MPa, $T_0 = 10$ °C. (a) $m = 0$ ppm, $\Delta P = 2.3$ MPa, $\varphi_0 = 15.5\%$; (b) $m = 0$ ppm, $\Delta P = 1.76$ MPa, $\varphi_0 = 17.4\%$; (c) $m = 100$ ppm, $\Delta P = 3.55$ MPa, $\varphi_0 = 13.6\%$; (d) $m = 400$ ppm, $\Delta P = 2.38$ MPa, $\varphi_0 = 17.0\%$.

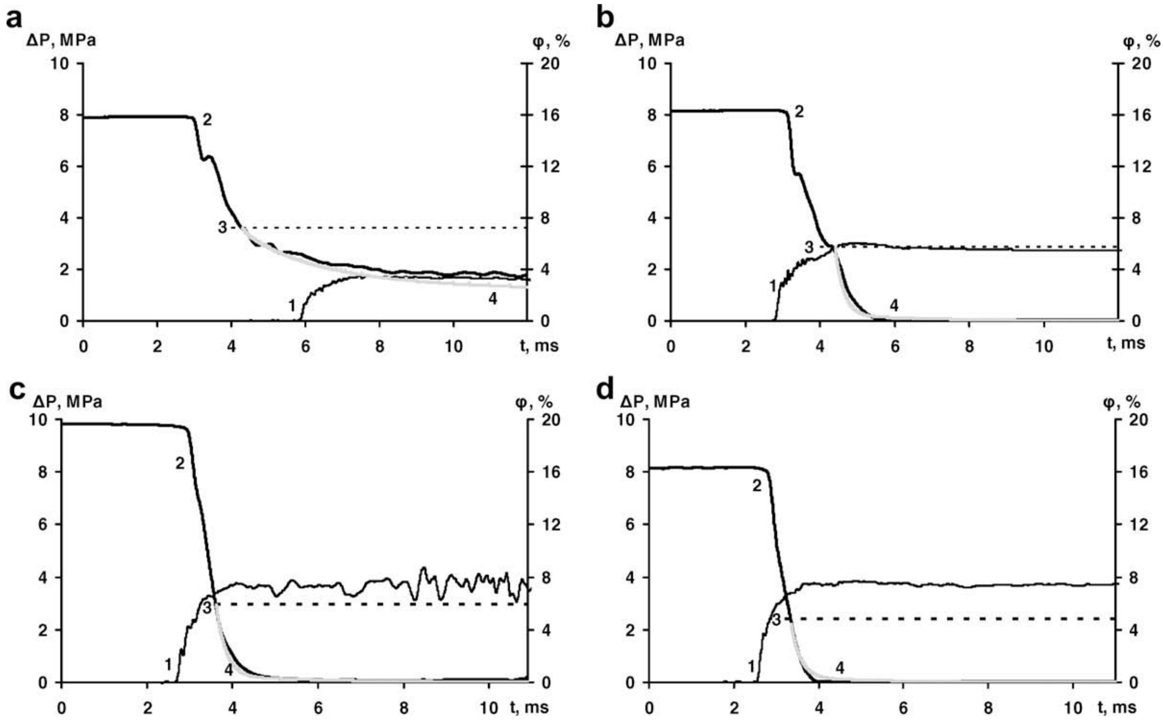

Fig. 5. Profiles of pressure shock wave and volumetric gas content in the wave in terms of gas dilution and hydration. $P_0 = 1.3$ MPa, $T_0 = 1$ °C. (a) $m = 0$ ppm, $\Delta P = 1.7$ MPa, $\varphi_0 = 15.7\%$; (b) $m = 0$ ppm, $\Delta P = 2.84$ MPa, $\varphi_0 = 16.3\%$; (c) $m = 100$ ppm, $\Delta P = 3.7$ MPa, $\varphi_0 = 19.4\%$; (d) $m = 400$ ppm, $\Delta P = 3.7$ MPa, $\varphi_0 = 16.3\%$.

2) at static pressure $P_0 = 1.3$ MPa, medium temperature $T_0 = 1$ °C and various mass concentrations of surfactant m in water (line 3 – isothermal compression of gas bubbles, line 4 – calculation according to the model). At the given temperature of gas and fluid medium beyond the shock wave hydrate forming is possible. Comparing experimental profiles of gas content for different values of surfactant concentration and close values of wave amplitude (Fig. 5c and d), we infer that presence of surfactant in the medium does not cause significant changes of gas content profiles and therefore, change in velocity of carbonic gas dilution in water.

Thus, at the given static pressure surfactant also does not speed up gas dilution process beyond the shock wave.

Comparing gas content profiles in Fig. 4 и 5 for close wave amplitudes we infer that temperature decrease from $T_0 = 10$ to 1 °C results in drastic increase of the velocity of changing gas content beyond the shock wave. Such significant decrease of volumetric gas content cannot be achieved only because of increased gas solubility but mainly caused by hydrate forming beyond the shock wave. Since dilution and carbonic gas hydrate forming beyond the shock wave have close values of velocity and time it is impossible to separate this process for the experiment.

Carried out calculations prove that portion of dissolved and hydrated carbonic gas beyond the shock wave front have the same order and allow separation of this process. Comparison of experimental gas content profiles (line 2) with calculation lines (line 4) shows that theoretical model rather well describes concurrent gas dilution process beyond the wave front – Fig. 5. In the calculation initial volumetric gas content in gas and fluid cluster was $\varphi_{cl} = 50\%$ for Fig. 5a and $\varphi_{cl} = 25\%$ for Fig. 5a–d. Concordance of calculated curves 4 with experimental profiles 2 for strong wave amplitudes (Fig. 5c and d.) signifies the prevailing role of hydrate forming over carbonic gas liquefaction beyond the shocking wave in gas and fluid medium.

Fig. 6 presents experimental data on volumetric gas content (points 1–6) for the studied time of the process beyond the shock wave front depending on the wave amplitude for different values of mass concentration of surfactants in the medium, temperature and initial static pressure in gas and fluid medium. φ_* – measured value of volumetric gas content in the time $t = 9$ ms beyond the shock wave. Experimental points in Fig. 6a correspond with the medium temperature $T_0 = 10$ °C, equal to critical temperature of carbonic gas hydrate forming. Therefore changing gas content is caused only by gas solubility. Points in Fig. 6b correspond with concurrent process of dilution and hydrate forming beyond the shock wave. We see that experimental points 1, 2, 3 for various concentration of surfactant at $P_0 = 0.5$ MPa (and points 4, 5, 6 at $P_0 = 1.3$ MPa) practically coincide for corresponding wave and medium parameters. This once again confirms that presence of surfactant has no influence on dilution and hydrate forming beyond the shock wave in gas and fluid mixture. Quite significant spread of experimental points is caused mainly by extended bar charts of sized bubble fragmentation that can significantly vary for different initial bubbles. Bubble fragmentation into small gas oscillations depends on the bubble size, its shape and orientation with regard to falling shock wave. If the initial size of specific bubble before fragmentation can be evaluated in accordance with the sizing bar charts of initial bubbles spread, their shape and orientation are free.

We see that with the increase of relative amplitude of shock wave, velocity of dilution and hydrate forming increase since relative volumetric gas content on the 9th ms beyond the shock wave front φ_*/φ_c decreases as $\Delta P/P_0$ grows at the constant P_0. Comparing experimental points 4, 5, 6 at $P_0 = 1.3$ MPa (and points 1, 2, 3 at $P_0 = 0.5$ MPa) in Fig. 6a and б we infer that medium temperature decrease results in decreased relative volumetric gas content for the given wave amplitude. This is caused by increased solubility of carbonic gas, decreased medium temperature and hydrate forming at $T_0 = 1$ °C.

In lines 7, 8 of Fig. 6 there is calculation on the proposed model at $\varphi_{cl} = 50\%$, and lines 9, 10 – $\varphi_{cl} = 25\%$. In the calculation radius of bubbles in cluster R changed with changing shock wave amplitude in accordance with the experiment. It is clear that lines 7, 8 in Fig. 6a quite well describe experimental data for corresponding values P_0. For static pressure in the medium $P_0 = 1.3$ MPa and shock wave amplitude $\Delta P/P_0 \geqslant 2$ except for the process of dilution at the given temperature carbonic gas liquefaction process is possible. Influence of this process may result in deviation of the experimental points (4–6) from the calculation line 8 at the wave amplitude $\Delta P/P_0 = 2.7 \div 2.8$ – Fig. 6a. Note, that variation of volumetric gas content in gas and fluid cluster φ_{cl} practically does not change calculation results for dilution beyond the shock wave.

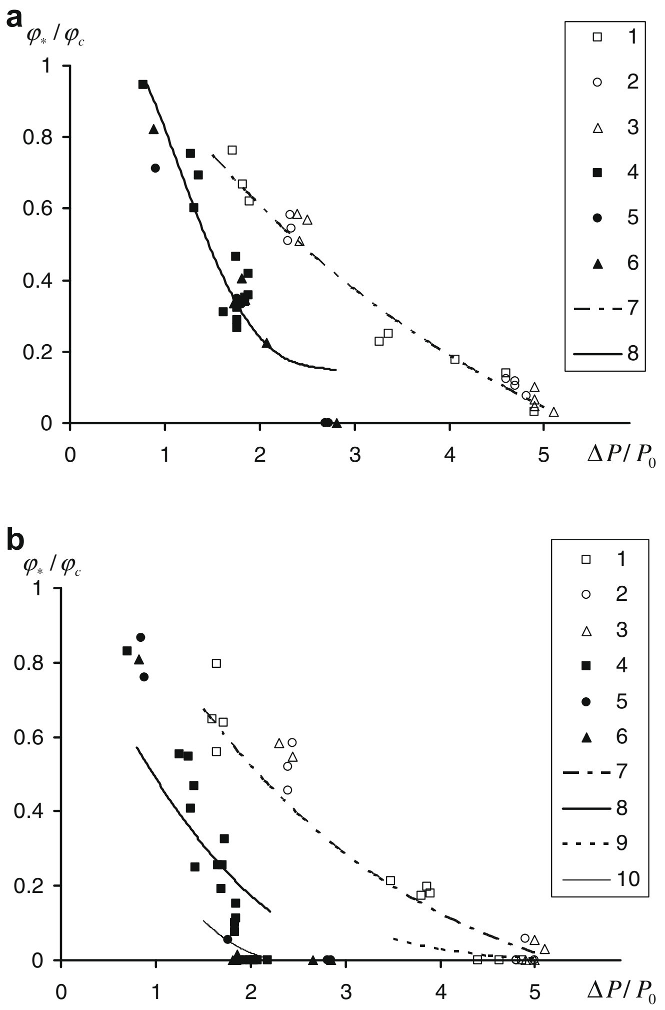

Fig. 6. Relative volumetric gas content beyond the shock wave front for studied time of the process ($t = 9$ ms). (a) –$T_0 = 10$ °C. $P_0 = 0.5$ MPa, $R_b = (0.03 - 0.15)$ mm: 1 – $m = 0$ ppm, 2 – 100 ppm, 3 – 400 ppm; $P_0 = 1.3$ MPa, $R_b = (0.03 - 0.30)$ mm: 4 – $m = 0$ ppm; 5 – 100 ppm; 6 – 400 ppm. (b) –$T_0 = 1$ °C, $P_0 = 0.5$ MPa, $R_b = (0.03 - 0.15)$ mm: 1 – $m = 0$ ppm; 2 – 100 ppm; 3 – 400 ppm; $P_0 = 1.3$ MPa, $R_b = (0.03 - 0.30)$mm: 4 – $m = 0$ ppm; 5 – 100 ppm; 6 – 400 ppm. 7–10 – calculation on the proposed model.

At the same time φ_{cl} has strong impact on calculation for hydrate forming beyond the shock wave – Fig. 6b. For static pressure in the medium $P_0 = 0.5$ MPa experimental data are in rather good accord with the calculation at $\varphi_{cl} = 50\%$. For the value $P_0 = 1.3$ MPa experimental data are set mainly between the calculated curves at $\varphi_{cl} = 50\%$ and $\varphi_{cl} = 25\%$. Decreasing wave amplitude should lead to the increase of φ_{cl} value in the calculation. Indeed, in the experiment as wave amplitude increases gas and fluid clusters amplify after bubble fragmentation that results in the decrease of φ_{cl}.

Fig. 7 presents experimental data (points 1–6) of dilution time τ_s – (a) and time of concurrent gas dilution and hydration τ_{h+s} – (b) beyond the shock wave in gas and fluid medium depending on its amplitude for different values of static pressure and surfactant concentration in the medium. Time domains in the experiments were set from the moment of isothermal compression of bubbles in the shock wave (point of intersection of isothermal compression line (line 3) with gas content profile

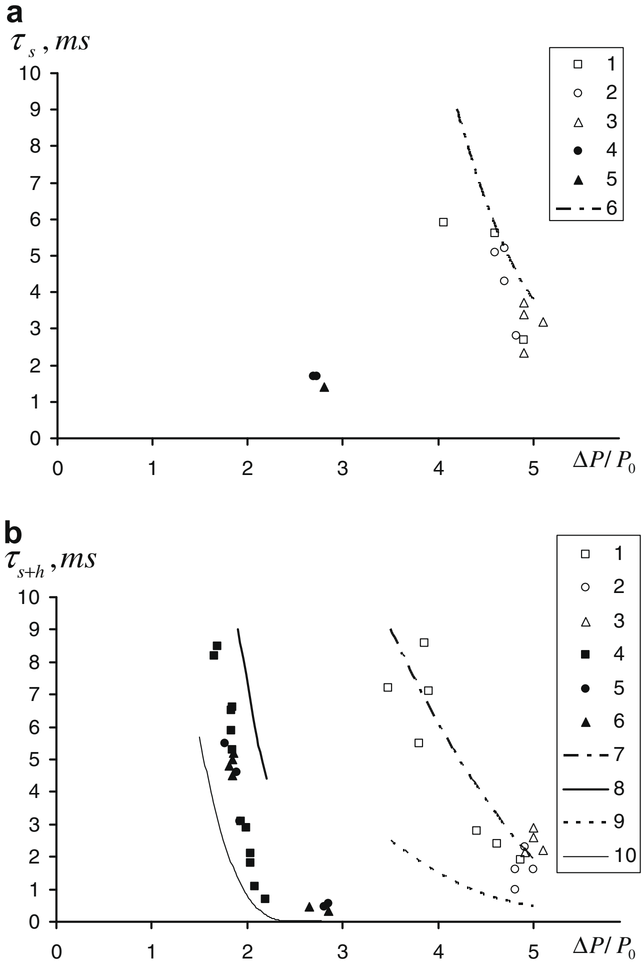

Fig. 7. Time of gas dilution and hydration beyond the shock wave front. (a) $-T = 10$ °C. $P_0 = 0.5$ MPa, $R_b = (0.03–0.15)$ mm: 1 – $m = 0$ ppm, 2 – 100 ppm, 3 – 400 ppm; $P_0 = 1.3$ MPa, $R_b = (0.03–0.30)$ mm: 4 – $m = 100$ ppm, 5 – 400 ppm. (b) $-T_0 = 1$ °C. $P_0 = 0.5$ MPa, $R_b = (0.03–0.15)$ mm: 1 – $m = 0$ ppm, 2 – 100 ppm, 3 – 400 ppm; $P_0 = 1.3$ MPa, $R_b = (0.03–0.30)$mm: 4 – $m = 0$ ppm, 5 –100 ppm, 6 – 400 ppm, 7–10 – calculation on the proposed model.

(line 2) in Figs. 2–5) to the level of $0.2 \cdot \varphi_c$. As shock wave amplitude grows dilution and hydration times decrease. This is connected with gas bubbles fragmentation and pressure growth beyond the shock wave front. Bubble fragmentation drastically decreases size of gas oscillations increasing interphase surface. Growing pressure beyond the wave front for hydration process increases overcooling degree beyond the shock wave according to equilibrium state and for dilution process increases diffusion force. Besides dilution and hydrate forming velocities will be determined by the velocity of heat removal from the boundary of gas bubbles.

Note that as well as for all previous experimental data presence of surfactant has no impact on dilution and hydrate forming – points 1, 2, 3 for $P_0 = 0.5$ MPa (4, 5, 6 for $P_0 = 1.3$ MPa) in Fig. 7 are not stratified.

Comparing experimental points for corresponding static pressures but for different temperatures of the medium in Fig. 7a and b we find that decrease of the medium temperature results in the decrease of dilution and hydration times for similar wave amplitudes that is conditioned mainly by the hydration process at $T_0 = 1$ °C, and also increased solubility of carbonic gas in water with the lower temperature of the medium.

Line 6 in Fig. 7a demonstrates the calculation on the proposed model at $\varphi_{cl} = 50\%$. It is evident that experimental time points of the dilution process at $P_0 = 0.5$ MPa can be well generalized by the calculation curve.

Lines 7, 8 in Fig. 7b demonstrates calculation on the proposed model at $\varphi_{cl} = 50\%$, and lines 9, 10 – $\varphi_{cl} = 25\%$. It is evident that experimental time points of the concurrent process of dilution and hydration at $P_0 = 0.5$ MPa are well generalized by the calculation curve for $\varphi_{cl} = 50\%$. Experimental data for $P_0 = 1.3$ MPa are between the calculation curves for $\varphi_{cl} = 50\%$ и $\varphi_{cl} = 25\%$.

Fig. 8 demonstrates calculation curves of volumetric parts of dissolved – 1, 3 and hydrated gas – 2, 4 beyond the shock wave front for various values of initial static pressure in the medium and initial volumetric gas content in gas and fluid cluster. It is apparent that as the wave amplitude grows share of hydrated gas increases. Accordingly, share of dissolved gas after reaching its maximum will decrease along with the wave amplitude growth. Calculations show that the value of initial volumetric gas content in gas and fluid cluster has weak impact on the dilution process beyond the shock wave – Fig. 8b, lines 1 and 3. At the same time decrease of initial volumetric gas content in the cluster results in significant increase of hydrated gas share – lines 2 and 4. Thus, calculation model unlike the experiment allows separating process of dilution and hydration of highly

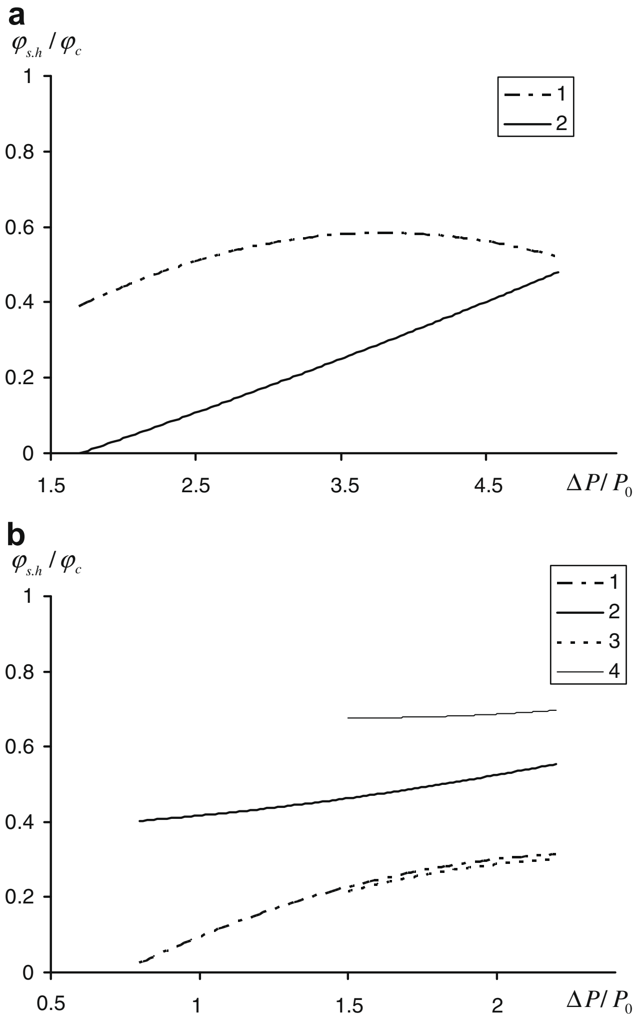

Fig. 8. Volume fraction of dissolved – 1, 3 and hydrated gas – 2, 4 beyond the wave front for the studied time of the process ($t = 9$ ms). $T = 1$ °C. (a) $P_0 = 0.5$ MPa, $R_b = (0.03–0.15)$ mm, $\varphi_{cl} = 50\%$; (b) $P_0 = 1.3$ MPa, $R_b = (0.03–0.30)$ mm: 1, 2 – $\varphi_{cl} = 50\%$; 3, 4 – $\varphi_{cl} = 25\%$.

soluble gases in water beyond the shock wave and studying these processes independently.

5. Conclusion

It has been shown that beyond the medium amplitude shock wave in fluid with carbonic gas bubbles there is intense process of dilution and hydrate forming resulting in complete disappearance of gas phase for several milliseconds. Presence of surfactant in the medium has no impact on dilution and hydration process beyond the shock wave in gas and fluid medium during studied time diapasons. As a result of the work we have received dependencies of dilution and hydrate forming times beyond the shock wave from the wave and medium parameters. Authors propose theoretical model of dilution and hydrate forming process beyond the shock wave in gas and fluid medium taking into account convective and molecular gas diffusion in fluid, convective and conductive heat exchange caused by heat generation in the interphase boundary. Close fit of experimental data and calculations has been achieved.

Acknowledgements

The work was carried out with the financial support from Russian Foundation of Fundamental Research (No. 06-08-00657) and RF President grant for governmental support of the leading scientific institutions (NS-3417.2008.8).

References

[1] N. Handa, T. Oshumi, Direct ocean disposal of carbon dioxide, Terrapub., Tokyo, 1995.

[2] V. Anderson, S. Woodhouse, O.Fr. Graff, J.S. Gudmundson, Hydrates for deep ocean storage of CO2, in: Proceedings of the Fifth International Conference on Gas Hydrates, June 13–16, Trondheim, Norway, 2005, pp. 1135–1139.

[3] S. Tanaka, F. Maruyama, O. Takano, et al., Experimental study on CO2 storage and sequestration in form of hydrate pellets, in: Proceedings of the Fifth International Conference on Gas Hydrates, Trondheim, Norway, June 13–16, 2005, pp. 1314–1319.

[4] S. Tanaka, O. Takano, K. Uchida, et al., Gas hydrate formation technology using low-temperature and low-pressure conditions. Part 2 – study on application to CO2 separation with a bench plant, in: Proceedings of the Fifth International Conference on Gas Hydrates, June 13–16, Trondheim, Norway, 2005, pp. 1332–1339.

[5] M. Ota, M. Seko, H. Endou, Gas separation process of carbon dioxide for mixed gases by hydrate production, in: Proceedings of the Fifth International Conference on Gas Hydrates, June 13–16, Trondheim, Norway, 2005, pp. 340–1343.

[6] R. Ohmura, S. Kashiwazaki, S. Shiota, et al., Structure-1 and structure-2 hydrate formation using water spraying, in: Proceedings of the Fourth International Conference on Gas Hydrates, May 19–23, Yakohama, Japan, 2002, pp. 1049–1054.

[7] K. Miyata, T. Oku, H. Hirayama, et al., A challenge to high-rate industrial production of methane hydrate, in: Proceedings of the Fourth International Conference on Gas Hydrates, May 19–23, Yakohama, Japan, 2002, pp.1031–1035.

[8] I.S. Gudmundsson, Method of obtaining gas hydrates for transportation and storage, Patent RF 2200727, C 07 C 5/02, No. 97112086/06, Appl. 02.07.1997, Publ. 20.03.2003, Bull. No. 8.

[9] V.S. Yakushev, Method of extraction and transportation of natural gas from gas and gas-hydrate sea-based deposits, called flowers and bees, Patent RF 2198285, E 21 B 43/01, No. 98113838/03, Appl. 13.07.1998, Publ. 10.02.2003, Bull. No. 4.

[11] K.B. Komissarov, V.A. Finochenko, Facility for obtaining gas hydrate, Patent RF 2045718, F 25 D 3/12, No. 5044706/13, Appl. 29.05.1992, Publ. 10.10.1995, Bull. No. 28.

[12] Y. Kozo, F. Tetsuro, K. Takahiro, K. Yuichi, Production method for gas hydrates and device for producing same, Pat. GB 2347938 A, C 07 C7/152, N 0006039.2., Publ. 20.09.2000.

[13] V.E. Dontsov, V.E. Nakoryakov, L.S. Chernoy, The method of gas hydrate production, Patent RF 2270053, C 2, No. 2003133051/15, Appl. 11.11.2003, Publ. 20. 02. 2006, Bull. No. 5.

[14] V.E. Nakoryakov, V.E. Dontsov, A.A. Chernov, Formation of gas hydrates in a gas–liquid mixture behind a shock wave, Doklady Phys. 51 (2) (2006) 621–624.

[15] V.E. Dontsov, V.E. Nakoryakov, A.A. Chernov, Shock waves in water with freon 12 bubbles and formation of gas hydrate, J. Appl. Mech. Tech. Phys. 48 (3) (2007) 346–360.

[16] V.E. Dontsov, A.A. Chernov, E.V. Dontsov, Shock waves and formation of carbon dioxide hydrate at an increased pressure in the gas–liquid medium, Thermophys. Aeromechan. 14 (1) (2007) 21–35.

[17] K. Watanabe, S. Imai, Y. Mori, Surfactant effects on hydrate formation in a unstirred gas/liquid system: an experimental study using HFC-32 and sodium dodecyl sulfate, in: Proceedings of the Fifth International Conference on Gas Hydrates, June 13–16, Trondheim, Norway, 2005, pp. 347–359.

[18] S. Sun, S. Fan, D. Liang, et. al., Ultrasonic experiment on hydrate formation of a synthesis gas, in: Proceedings of the Fifth International Conference on Gas Hydrates, June 13–16, Trondheim, Norway, 2005, pp. 394–397.

[19] N. Gnanedran, R. Amin, Therodynamic and kinetic modelling of a hydrate promoter–water–gas system in a spray reactor, in: Proceedings of the Fifth International Conference on Gas Hydrates, June 13–16, Trondheim, Norway, 2005, pp. 384–393.

[20] T. Daimaru, Y. Kuji, Y. Yanagisawa, A. Tamasaki, Effect of the structure of surfactants on the hydrate formation kinetics of methane and xenon – effect of the carbon chain length, in: Proceedings of the Fifth International Conference on Gas Hydrates, June 13–16, Trondheim, Norway, 2005, p. 1022.

[21] K. Okutani, Y. Kuwabara, Y. Mori, Surfactant effect on hydrate formation in an unstirred gas/liquid system: an experimental study using methane and sodium alkyl sulfates, Chem. Eng. Sci. 63 (2008) 183–194.

[22] V.A. Istomin, V.S. Yakushev, Gas Hydrates in Nature, Nedra, Moscow, 1992.

[23] R.I. Nigmatulin, Dynamics of Multiphase Media, Hemisphere Publ., New York, 1991.

[24] S.S. Kutateladze, V.E. Nakoraykov, Heat and Mass Transfer and Waves in a Gas-Liquid Systems, Nauka, Novosibirsk, 1984.

[25] Reference Book of Solubility, Academy Science of USSR, vol. 1, Moscow, Leningrad, 1961.

[26] Yu. F. Makogon, Hydrates of Hydrocarbons, Pennwell Pub. Comp., Tulsa, Oklahoma, 1997.

[27] T. Hobler, Mass Transfer and Absorption, Chemistry, Leningrad, 1964.

[28] M. Hozawa, M. Inoue, J. Sato, et al., Marangoni convection during steam absorption into aqueous Li Br solution with surfactant, J. Chem. Eng. Jpn. 24 (2) (1991) 209–214.